GSA Data Repository 2017074

Forecasting Transitions in Monogenetic Eruptions Using the Geologic Record

Gábor Kereszturi[1*] – Mark Bebbington[1,2] – Károly Németh[1]

Supplementary File: Data and Statistical Modelling Details

Table DR1. Data and fitted transition probabilities.

ID	Volcano name	$\overline{A}$ (ky)	A_{ph} (km^2)	V_{ph} (10^6 m^3)	Substrate (H sandstone, S sand)	T_S (m)	Z (m asl)	$Z_{\overline{A}}$ (m apsl)	D_f (m)	TRANS	$\hat{p}$
1	Onepoto Basin	247	0.76	2.62	H	0	0	50	690	0	0.177 ± 0.182
2	Albert Park	227	1.19	2.29	H	10	28	88	1,160	1	0.766 ± 0.172
3	Boggust Park	204	0.37	0.32	S	37	5	23	3,259*	0	0.031 ± 0.084
4	Pupuke	200	3.14	26.47	H	0	0	15	1,463	1	0.837 ± 0.126
5	Pukewairiki	199	1.03	3.34	S	23	0	18	2,317*	1	0.790 ± 0.210
6	Waitomokia	194	0.89	3.33	S	39	0	60	3,547*	1	0.736 ± 0.230
7	St. Heliers	180	0.39	2.20	H	0	24	112	368	0	0.565 ± 0.209
8	Te Pou Hawaiki	153	1.13	3.39	H	16	75	180	1,287	1	0.967 ± 0.042
9	Pukeiti	114	N/A	N/A	S	36	18	48	3,572*	1	0.885 ± 0.165
10	Orakei Basin	103	1.74	6.70	H	15	0	40	198	0	0.514 ± 0.179
11	Pukaki	84	2.48	9.19	S	60	0	40	1,185	0	0.217 ± 0.249
12	Tank Farm	70	1.00	5.51	H	5	45	120	340	0	0.972 ± 0.032
13	Grafton	70	1.20	5.51	H	5	52	127	665	1	0.988 ± 0.018
14	Auckland Domain	70	1.20	5.51	H	5	52	127	665	1	0.988 ± 0.018
15	Mt. St. John	55	N/A	N/A	H	0	53	133	444	1	0.984 ± 0.025
16	Maungataketake	41.4	2.58	7.25	S	35	0	80	3,425*	1	0.982 ± 0.051
17	Otuataua	41.4	N/A	N/A	S	35	17	97	3,561*	1	0.961 ± 0.098
18	McLennan Hills	40.1	1.09	1.89	S	23	3	83	638	1	0.992 ± 0.014
19	One Tree Hill	35	N/A	N/A	H	0	55	145	1,320	1	0.997 ± 0.008
20	Kohuora	34	1.92	7.24	S	48	6	96	2,469*	0	0.597 ± 0.329
21	Browns Island	33.8	0.72	0.97	H	0	-2	93	160	1	0.401 ± 0.275
22	Mt. Albert	32.8	0.92	1.82	H	1	56	151	130	1	0.968 ± 0.033
23	Ash Hill	32.3	0.25	0.08	S	23	0	95	156	0	0.002 ± 0.023
24	Hopua	32.2	0.35	0.86	H	17	0	95	98	0	0.467 ± 0.243
25	Cemetery Hill	32.1	0.19	0.24	S	55	20	115	1,963*	0	0.018 ± 0.063
26	Puketutu	31.9	1.52	4.47	S	26	0	100	2,711*	1	0.988 ± 0.041
27	Wiri Mountain	31.9	0.67	0.42	S	34	0	100	150	1	0.291 ± 0.249
28	Mt. Richmond	31.7	1.21	2.64	S	20	10	110	806	1	0.996 ± 0.008
29	Taylors Hill	31.7	0.48	3.97	H	7	25	125	778	1	0.996 ± 0.009
30	Crater Hill	31.6	1.57	7.65	S	58	0	100	872	1	0.678 ± 0.281
31	North Head	31.2	0.17	2.59	H	0	-2	98	2,450	1	0.984 ± 0.036
32	Panmure Basin	31.2	2.38	7.14	H	15	0	100	1,117	1	0.992 ± 0.015
33	Mt. Victoria	31.1	N/A	N/A	H	0	0	100	1,377	1	0.978 ± 0.062
34	Mt. Cambria	31.1	N/A	N/A	H	0	6	106	1,729	1	0.993 ± 0.027
35	Robertson Hill	31.1	2.17	2.48	S	26	10	110	2,409*	1	0.985 ± 0.045
36	Mt. Roskill	30.4	0.43	1.48	H	12	52	157	553	1	0.994 ± 0.011
37	Three Kings	28.8	2.16	6.44	H	5	37	147	340	1	0.992 ± 0.013
38	Mt. Hobson	28.6	N/A	N/A	H	5	74	184	397	1	0.993 ± 0.014
39	Mt. Eden	28.4	N/A	N/A	H	5	65	175	1,065	1	0.998 ± 0.007
40	Little Rangitoto	27.8	N/A	N/A	H	5	40	150	136	1	0.970 ± 0.040
41	McLaughlin Mt.	27.1	0.40	0.55	S	43	5	115	481	1	0.777 ± 0.176
42	Pigeon Mountain	26.8	0.92	2.29	H	23	14	129	92	1	0.930 ± 0.058
43	Mangere Lagoon	26.2	0.70	2.03	H	53	0	115	2,270*	1	0.943 ± 0.107
44	Hampton Park	25.3	0.63	0.36	S	17	19	134	2,232	1	0.915 ± 0.126
45	Otara Hill	25.3	0.86	0.66	S	17	25	140	1,822	1	0.992 ± 0.017
46	Green Hill	23.4	1.03	1.83	S	14	23	138	1,560	1	0.998 ± 0.005
47	Mt. Mangere	22.1	N/A	N/A	S	42	0	115	1,600*	1	0.961 ± 0.100
48	Mt. Smart	21.3	0.28	1.47	H	23	15	135	708	1	0.994 ± 0.011
49	Styaks Swamp	17.1	0.58	0.37	S	11	10	120	1,183	0	0.898 ± 0.141
50	Purchas Hill	10.8	0.54	1.66	H	10	31	51	874	1	0.998 ± 0.005
51	Mt. Wellington	10.5	0.65	3.4	H	10	22	42	314	1	0.995 ± 0.011
52	Rangitoto	0.5	1.13	7.36	H	15	-3	-3	3,313*	1	0.978 ± 0.066

Table DR1 presents the dataset used in the paper. The mean estimated age $\bar{A}$ is from the model proposed by Bebbington and Cronin (2011) and Bebbington (2013). The area (A_{ph}) and volume (V_{ph}) of phreato-magmatic deposits were measured by Kereszturi et al. (2013). The substrate type in the Auckland Volcanic Field is either the East Coast Bays Formation (alternating sandstone and mudstone), denoted by H, or the covering soft sediment of mud, sand and gravel, denoted by S. The estimated thickness of soft sediments is given by T_S. The present elevation above sea level is Z, while correcting for this using the mean estimated age and sea-level records (Kereszturi et al., 2014) gives a secondary covariate $Z_{\bar{A}}$. The distance to the nearest fault is given by D_f, where the asterix denotes a maximum distance; in some cases (*), due to overlaying sediment, there may be an unknown nearer fault. Whether the eruption made the transition to effusive is indicated by a 1 in the TRANS column.

In the southern parts of the Auckland Volcanic Field (AVF) the faults locations are not completely known due to burial by soft-sediments covering the hard basement rocks (e.g. Fig. DR1-3). Hence, for volcanoes located in the southern part of the AVF (denoted by an asterix in Table DR1) the presence of unknown faults means that the distance to the nearest (known) fault was treated as a maximum in the modeling procedure to remove the consequent bias. To achieve this, the distance to the nearest fault was modeled by a gamma distribution with density

$$f(x) = \frac{\beta^{\alpha} x^{\alpha-1} \exp(-\beta x)}{\Gamma(\alpha)}$$

This means that $y=1/x$ will have an inverse gamma density as:

$$f(y) = \frac{x^{-\alpha-1} \exp(-\beta^{-1}/y)}{\beta^{\alpha}\Gamma(\alpha)}$$

where the parameters α and β can be estimated using the Kaplan-Meier (Product Limit) estimate (see, e.g., Lawless 2003, p. 80), which allows for values for which only a *minimum* value is known; hence the inverse transformation. The Kaplan-Meier and fitted inverse gamma distribution for the distance to the nearest fault is shown in Figure DR1.

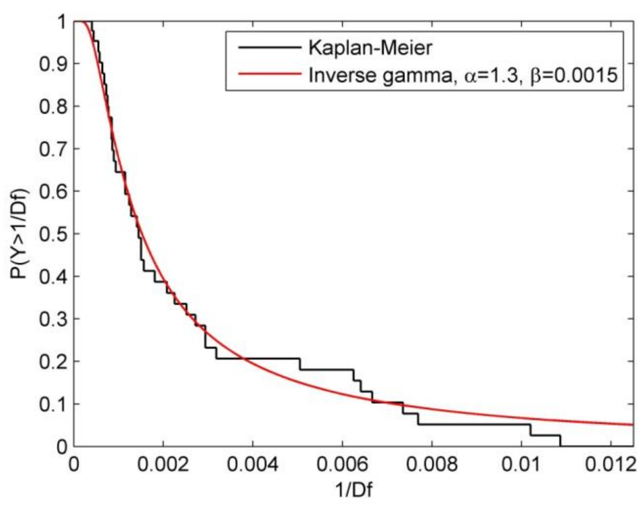

Figure DR1: Fitted distribution for unknown distances to faults.

When forecasting the likelihood of transition during a future eruption at locations in areas where we suspect buried faults, we use the median of the conditional distribution given the known maximum distance to a fault. In other words, we use D_{med}, which is the solution of the equation

$$\gamma(0.0015D_{\text{med}}, 1.3) = 0.5\gamma(0.0015D_{\text{max}}, 1.3)$$

where $\gamma(x,\alpha) = \int_0^x e^{-t}t^{\alpha-1}dt$ is the incomplete gamma function. The conversion from D_{max} to D_{med} is shown in Figure DR2.

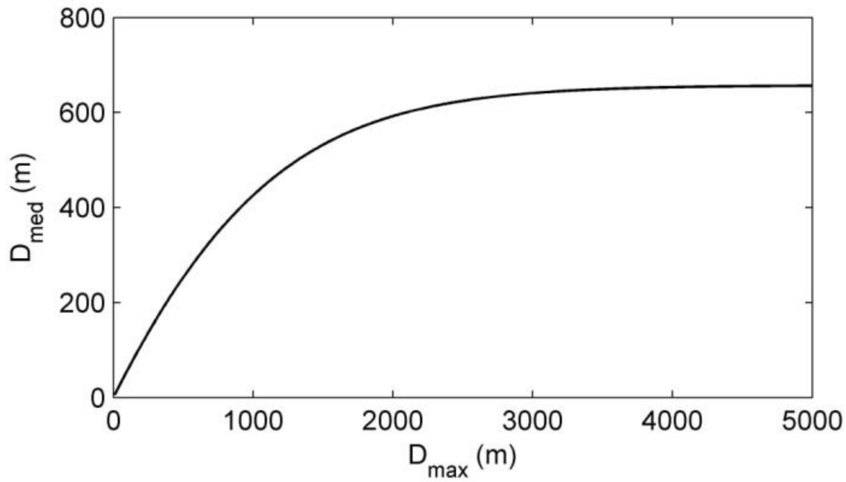

Figure DR2: Estimated distance to fault in the presence of unknown faults.

In several cases (e.g., N/A in Table DR1), no phreatomagmatic deposits were identifiable, due to erosion or burial by later deposits. This does not mean that these eruptions had no phreatomagmatic phase, and as these eruptions all, by definition, made the transition omitting them would bias our results. It is considered that all eruptions in the AVF have/will have a phreatomagmatic phase. From a modelling point of view, we want to avoid inferring any causality from the magmatic transition to unknown phreatomagmatic volumes or areas. Instead we use the empirical distribution of the phreatomagmatic volumes from the other volcanoes in the field, which avoids adding extra information, and still allows these eruptions to contribute toward the identification of geologic factors. Hence the missing data are imputed at each update from a gamma distribution fitted to the known (i.e., from the remaining 42 centres in Table DR1) volumes (α = 1.062, β = 0.2822) or areas (α = 2.311, β = 2.157).

The best model is the one with the smallest Deviance Information Criterion (DIC) value (Spiegelhalter et al., 2002). This balances model fit against model complexity. In this case, the model (note the absence of an intercept term) with minimum DIC = 32.201 was:

$$\log\frac{p}{1-p} = \beta_1\sqrt{A} + \beta_2 \log D_{\text{f}} + \beta_3 \mathrm{I_H} V_{\text{ph}}^{-0.25}(Z+5)^{-0.5} + \beta_4 \mathrm{I_S} V_{\text{ph}}^{-1} + \beta_5 \mathrm{I_S} \exp(T_s/10)$$

where p is the probability of transition, and $\mathrm{I_H}$ and $\mathrm{I_S}$ are indicator variables. The former equals 1 when the substrate is stone, 0 otherwise, while the latter equals 1 where the substrate is sand and mud, and is 0 elsewhere. Thus the first two terms are always present, while either the third or the fourth and fifth are present depending on the substrate. The addition of 5m to the elevations in the third term ensures that the term is monotonic in the phreatomagmatic volume, e.g., that a trend for a less likely transition with greater volumes does not change sign if the elevation increases. The factor of 10 in the fifth term is simply a rescaling.

The model was run for 50,000 iterations, plus a 1000 iteration burn-in period to overcome initial bias, and the remainder thinned by a factor of 10 to remove autocorrelations and produce an approximately random sample of size 5000. Using N(0,106) reference priors (Christensen et al., 2010), the estimated regression parameters are β_1 = -0.694 ± 0.317, β_2 = 1.908 ± 0.733, β_3 = -10.74 ± 4.96, β_4 = -2.675 ± 1.302, β_5 = -0.0226 ± 0.0093, all significant by DIC measure, with Prob($\beta_1 < 0$) = 0.9997, Prob($\beta_2 > 0$) = 0.9999, Prob($\beta_3 < 0$) = 0.9935, Prob($\beta_4 < 0$) = 0.9999, Prob($\beta_5 < 0$) = 0.9990.

The mapping (Fig 1 A&B) using Eq. 1 in the paper was performed using the input layers summarized in Fig. DR3-6. The factors are the distance from faults (Fig. DR3), present-day elevation (Fig. DR4), thickness of soft-sediment cover (Fig. DR5), and the substrate-type (Fig. DR6). Data on sediment thickness and fault lineaments in subaqueous areas is scarce, and so potential locations that are covered by sea are not included. Note that data on fault locations in the southern part of the AVF is uncertain, so the transition probability may be slightly higher or lower than is estimated through the bias correction above.

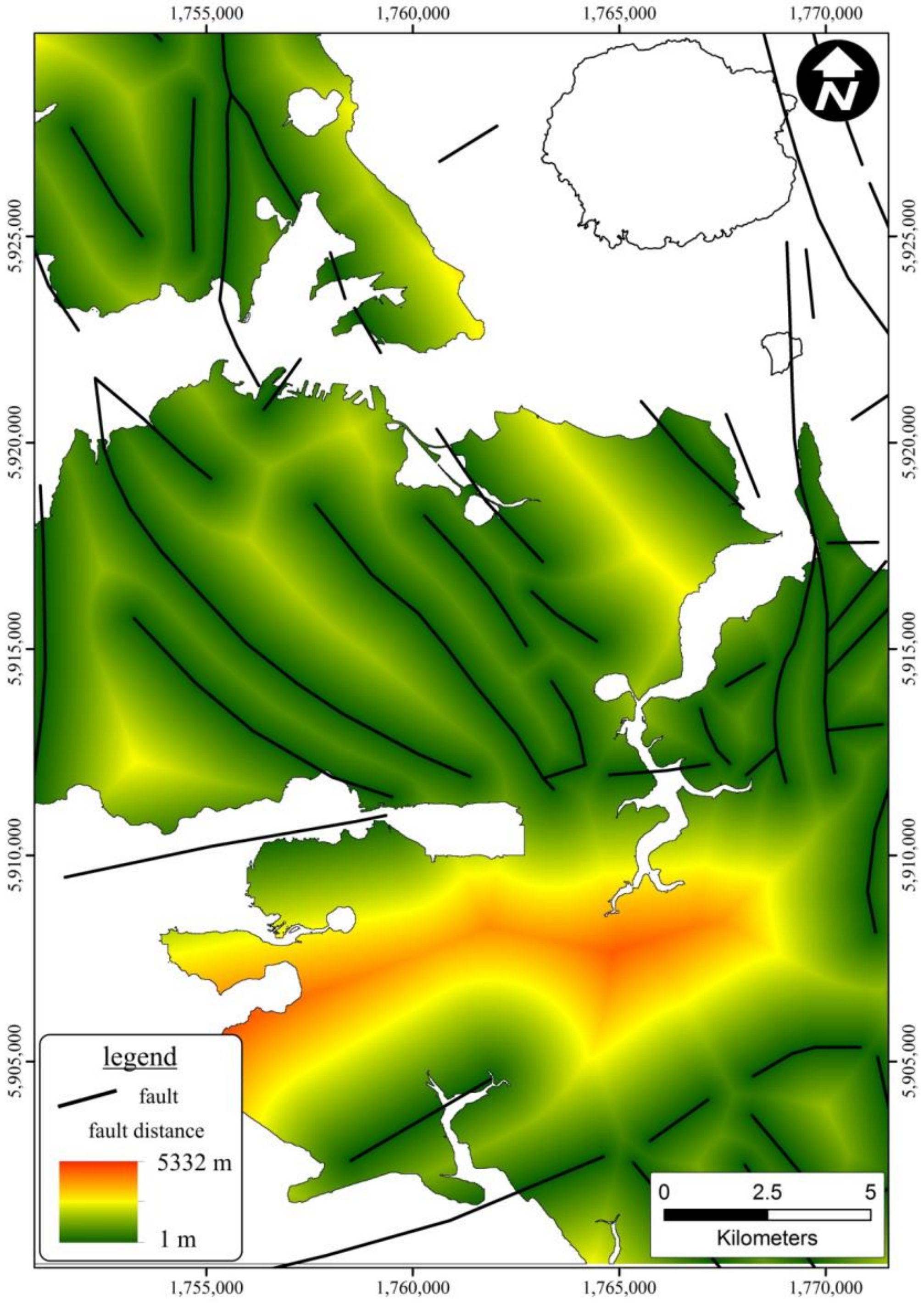

Fig. DR3: Distance from known faults. The fault data is after Kenny et al. (2012). The larger values in the southern part of the AVF suggest a bias due to soft-sediment cover.

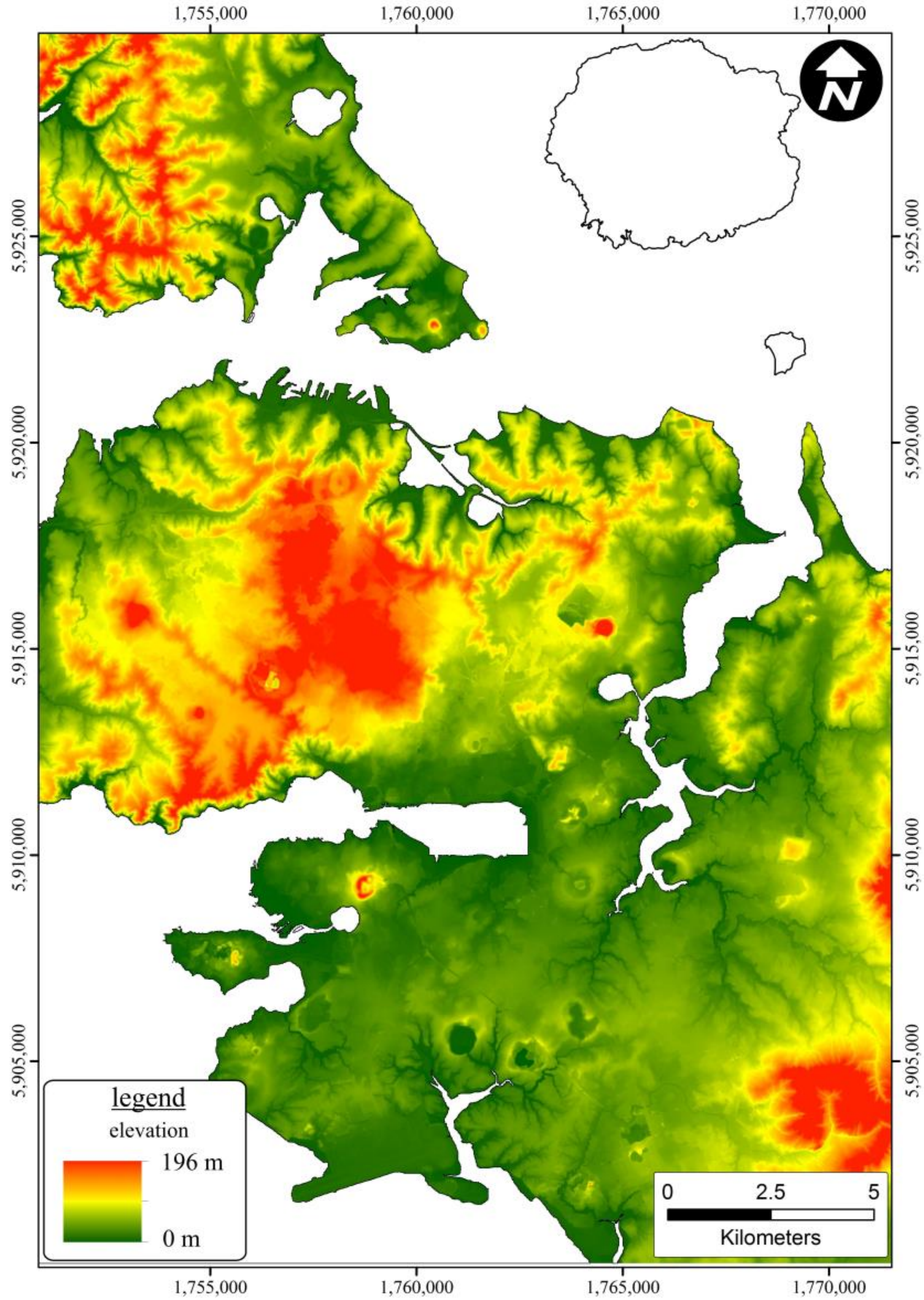

Fig. DR4: Elevation represented by Light Detection and Ranging (LiDAR) based Digital Terrain Model.

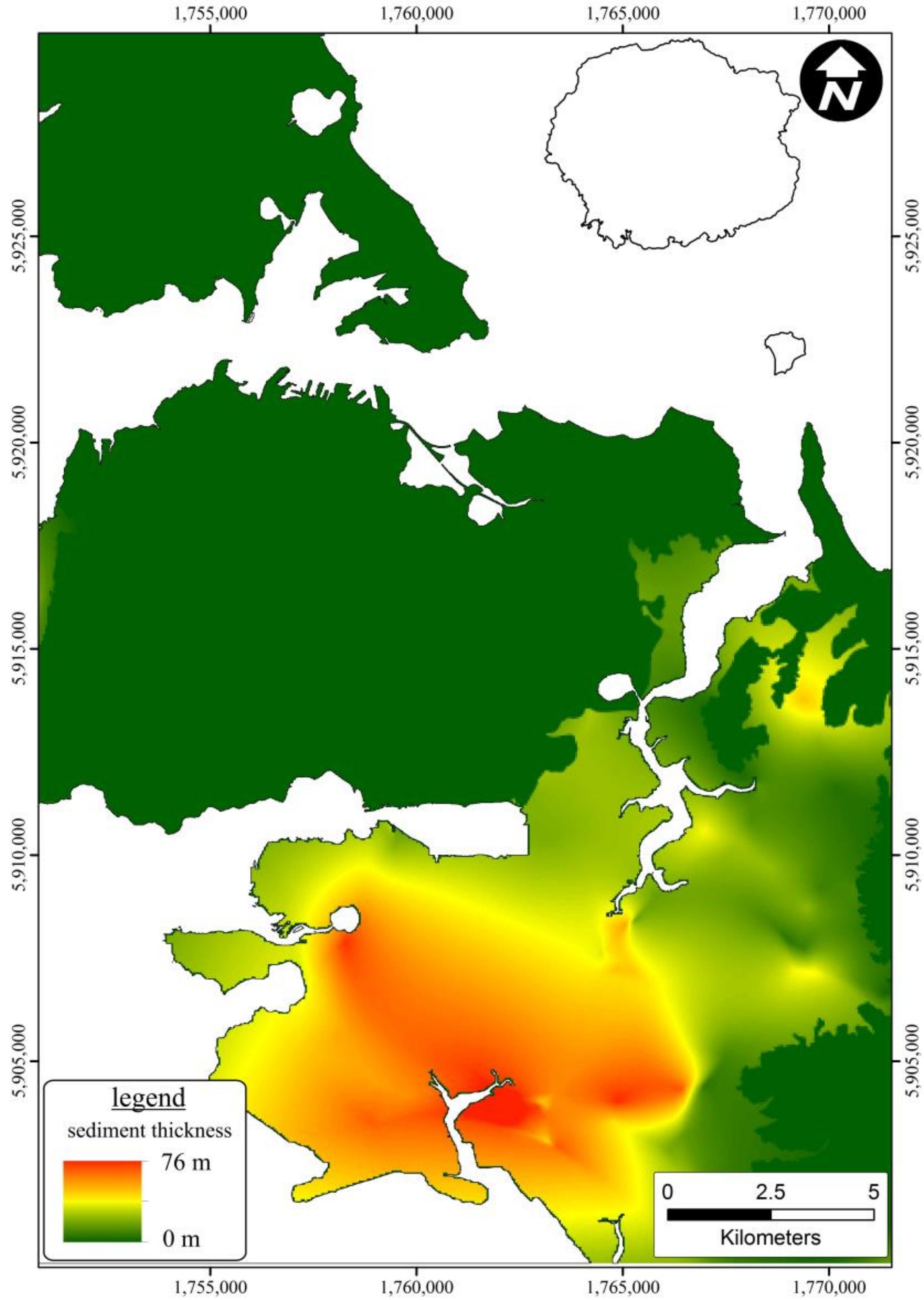

Fig. DR5: Thickness map of the semi- to unconsolidated-soft sediments in the AVF.

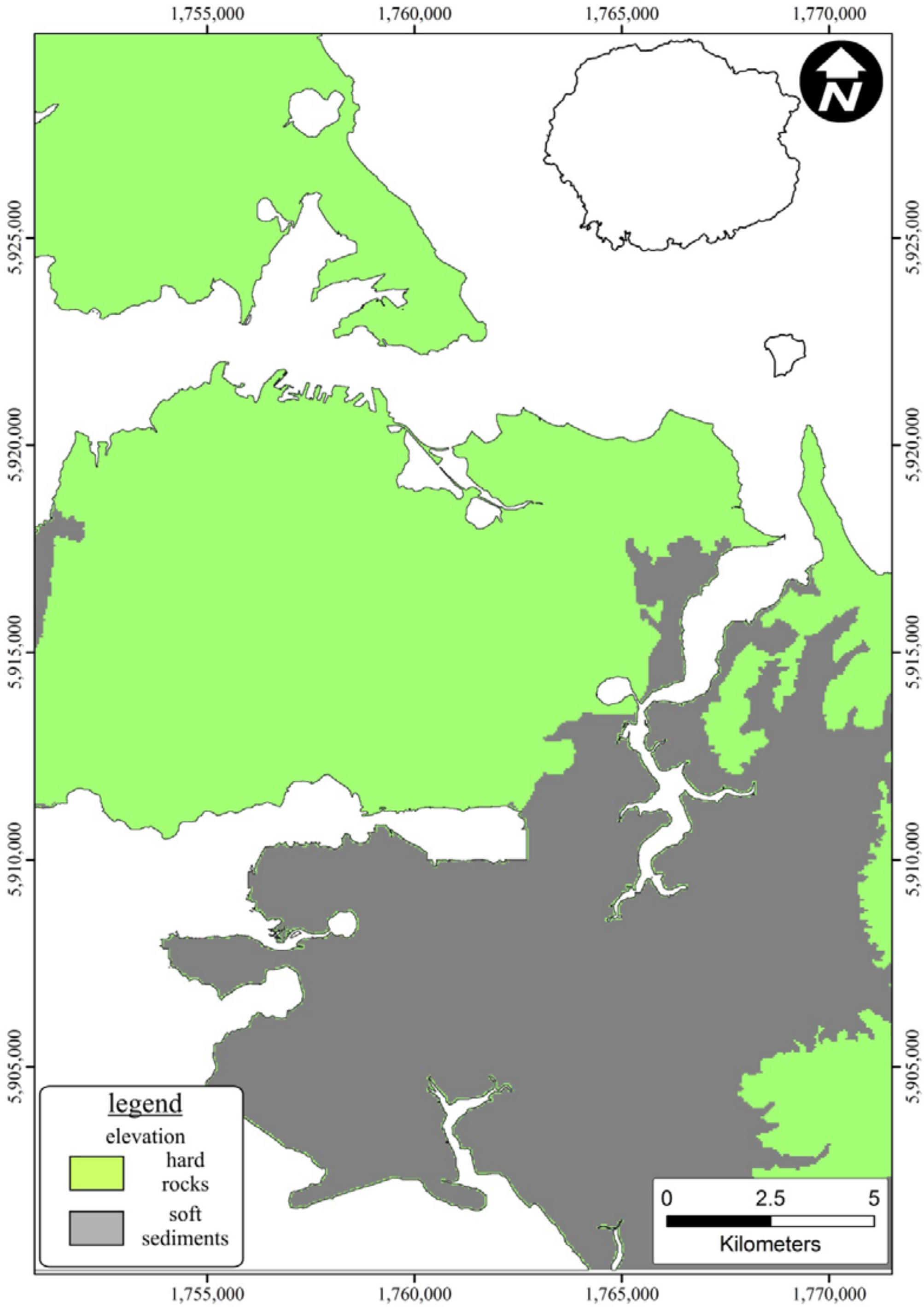

Fig. DR6: Substrate type in the AVF.

References

Bebbington, M.S., 2013, Assessing spatio-temporal eruption forecasts in a monogenetic volcanic field: Journal of Volcanology and Geothermal Research, v. 252, p. 14-28.

Bebbington, M.S., and Cronin, S.J., 2011, Spatio-temporal hazard estimation in the Auckland Volcanic Field, New Zealand, with a new event-order model: Bulletin of Volcanology, v. 73, p. 55-72.

Christensen, R., Johnson, W., Branscum, A., and Hanson, T.E., 2010, Bayesian Ideas and Data Analysis: An Introduction for Scientists and Statisticians: Boca Raton, Florida, CRC Press, Taylor & Francis Group, 516 p.

Kenny, J.A., Lindsay, J.M. and Howe, T.M., 2012. Post-Miocene faults in Auckland: insights from borehole and topographic analysis. New Zealand Journal of Geology and Geophysics, 55(4): 323-343.

Kereszturi, G., Németh, K., Cronin, S.J., Procter, J., and Agustín-Flores, J., 2014, Influences on the variability of eruption sequences and style transitions in the Auckland Volcanic Field, New Zealand: Journal of Volcanology and Geothermal Research, v. 286, p. 101-115.

Kereszturi, G., Németh, K., Cronin, S.J., Agustín-Flores, J., Smith, I.E.M., and Lindsay, J., 2013, A model for calculating eruptive volumes for monogenetic volcanoes — Implication for the Quaternary Auckland Volcanic Field, New Zealand: Journal of Volcanology and Geothermal Research, v. 266, p. 16-33.

Lawless, J.F., 2003, Statistical Models and Methods for Lifetime Data. Second Edition, Wiley, Hoboken, NJ

Spiegelhalter, D.J., Best, N.G., Carlin, B.P., and Van Der Linde, A., 2002, Bayesian measures of model complexity and fit: Journal of the Royal Statistical Society. Series B, Statistical Methodology, v. 64, p. 583–639, doi:10.1111/1467-9868.00353.